

# Multi-EM systems inversion - Towards a common conductivity model for the Tli Kwi Cho complex

Dominique Fournier\*, Lindsey Heagy, Nate Corcoran, Devin Cowan, Sarah G. R. Devriese, Daniel Bild-Enkin, Kristofer Davis, Seogi Kang, Dave Marchant, Michael S. McMillan, Michael Mitchell, Gudni Rosenkjar, Dikun Yang and Douglas W. Oldenburg, Geophysical Inversion Facility, University of British Columbia

## SUMMARY

The magnetic and electromagnetic responses from airborne systems at Tli Kwi Cho, a kimberlite complex in the Northwest Territories, Canada, have received considerable attention over the last two decades but a complete understanding of the causative physical properties is not yet at hand. Our analysis is distributed among three posters. In the first we find a 3D magnetic susceptibility model for the area; in the second we find a 3D conductivity model; and in the third we find a 3D chargeability model that can explain the negative transient responses measured over the kimberlite pipes.

In this second paper we focus upon the task of finding a conductivity model that is compatible with three airborne data sets flown between 1992 and 2004: one frequency-domain data set (DIGHEM) and two time-domain systems (AeroTEM and VTEM). The goal is to obtain a 3D model from which geologic questions can be answered, but even more importantly, to provide a background conductivity needed to complete the 3D IP inversion of airborne EM data. We begin by modifying our pre-existing 1D frequency and time domain inversion codes to produce models that have more lateral continuity. The results are useful in their own right but we have also found that 1D analysis is often very effective in bringing to light erroneous data, assisting in estimating noise floors, and providing some starting information for developing a background model for the 3D EM inversion. Here we show some results from our Laterally Constrained Inversion (LCI) framework. The recovered conductivity models seem to agree on the general location of the kimberlite pipes but disagree on the geometry and conductivity values at depth. The complete 3D inversions in time and frequency, needed to resolve these issues, are currently in progress.

## INTRODUCTION

The Tli Kwi Cho (TKC) kimberlite complex provides a classic example of the challenges faced in the integration of multiple data sets in exploration geophysics. The diamondiferous deposit is hosted within granitic and metamorphosed-mafic rocks of the Archean Slave Province, Northwest Territories, Canada, known to be dense and highly resistive rocks (Lord and Barnes, 1954; Coopersmith et al., 2006) (Figure-1). An airborne frequency domain survey (DIGHEM) flown in 1992 indicated two distinct kimberlite pipes, later confirmed by drilling and named DO-18 and DO-27. The TKC complex is partially covered by a conductive 5 to 50 m thick glacial till layer (Doyle et al., 1999). Subsequent airborne and ground-based surveys, including HLEM, TEM, VLF, magnetic and gravity surveys, were carried out in order to confirm the geometry and extent of the pipes and associated geological structures (Jansen

and Witherly, 2004). Physical properties were also measured on rock samples, confirming that both kimberlite pipes are weakly magnetic and of lower density than the background rocks (Doyle et al., 1999). The negative transient response measured over DO-18 and DO-27 by the time-domain EM system may suggest the pipes are also chargeable. There have been several studies focusing on individual data sets, each yielding slightly different interpretations (Boyko et al., 2000; Reed and Witherly, 2007). These variations in recovered conductivity distributions are in part the motivation for our research. Our goal is to find a single conductivity model that can explain all the data sets collected over the TKC complex. This model will then be used as a background model in a subsequent inversion of airborne IP data. We approach this challenge by considering a combined inversion strategy.

We focus our efforts on three airborne EM data sets: a frequency-domain DIGHEM (1992), a time-domain AeroTEM and a VTEM (2004) survey. All three data sets show strong EM responses over the kimberlites pipes. By integrating all available information, we aim to improve the conductivity inversion results and increase our overall understanding of the TKC complex.

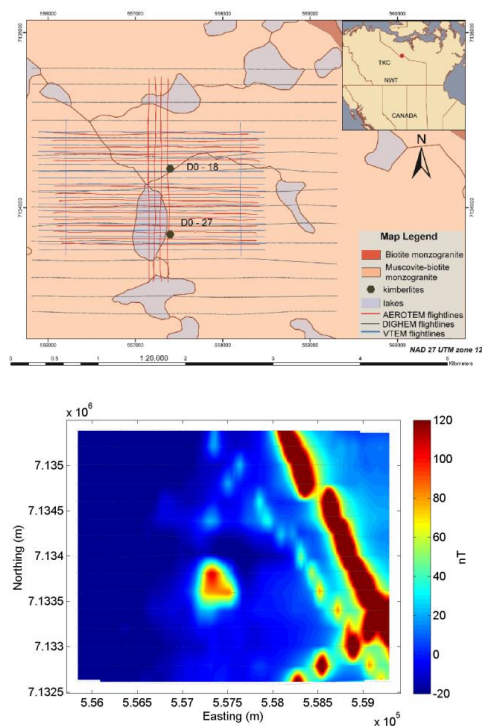


Figure 1: (a) Regional geology over the TKC area and (b) TMI data from the DIGHEM system.

## Multi-EM systems inversion: Tli Kwi Cho complex

### FREQUENCY DOMAIN EM DATA

A frequency domain EM survey (DIGHEM) was collected in 1992. The DIGHEM system measures five frequencies ranging from 900–56k Hz. The three highest frequencies are measured using a horizontal coplanar (HCP) transmitter-receiver configuration. The two lowest frequencies are vertical coaxial (VCA) loops. The survey lines were flown N90°E with 200 m line spacing and measuring every 10 m along line. The receiver measures both the in-phase and quadrature components in *ppm* of the secondary magnetic field normalized by the free-space magnetic field.

Figure 2 shows the interpolated data collected from the coplanar orientation at 900 Hz. Both kimberlite pipes have a strong quadrature component, indicative of highly conductive bodies. A strong negative response striking N30°W is seen on the in-phase component, corresponding to the location of a susceptible body as seen in Figure 1. Strong susceptible bodies are likely to influence the EM response over the area. Information from the TMI data set should be incorporated into future inversions.

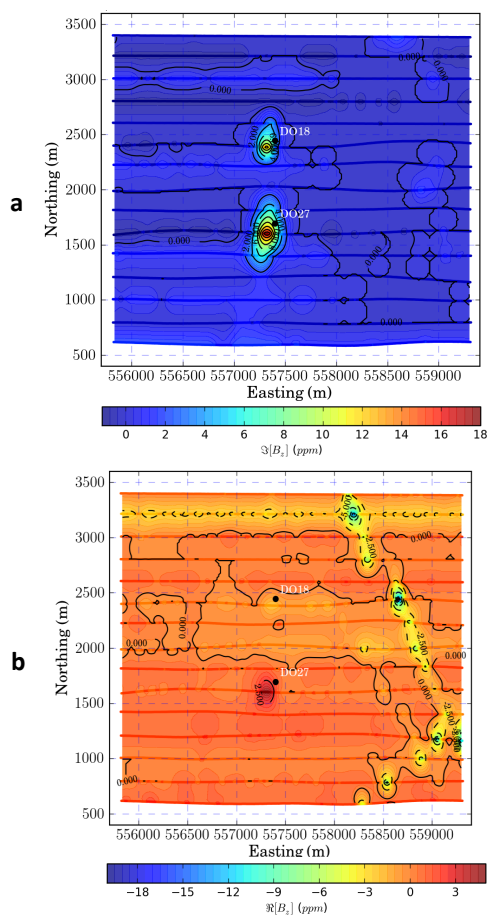


Figure 2: Interpolated (a)  $\Im[B_z]$  and (b)  $\Re[B_z]$  components at 900 Hz from the DIGHEM data set.

### TIME DOMAIN EM SYSTEMS

An airborne time-domain survey (AeroTEM) was flown in 2003 by Aeroquest. A total of 19 lines were surveyed at 75 m separation, measuring every 3 m along line (Figure 3a). The AeroTEM system uses a triangular waveform, recording 16 on-time channels and 17 off-time channels. Observations of the time-varying vertical magnetic fields are measured in nano-Tesla per second. A second time-domain survey (VTEM) was flown in August 2004 by Geotech. A total of 20 lines oriented N90°E were collected at 75 m line spacing, at a 10 Hz sampling frequency. The VTEM system uses a trapezoidal waveform and measures the *z*-component of  $\frac{\partial B}{\partial t}$  on 27 off-time channels. Figure 3(b) shows the VTEM data collected at an early time.

Both time-domain data sets measured negative transient responses in the vicinity of DO-18 and DO-27. Negative EM responses may be due to IP effects as suggested by Weidelt (1982). Current airborne EM inversion algorithms cannot account for IP effects, hence the inverted models presented in the following section will assume frequency independent conductivity.

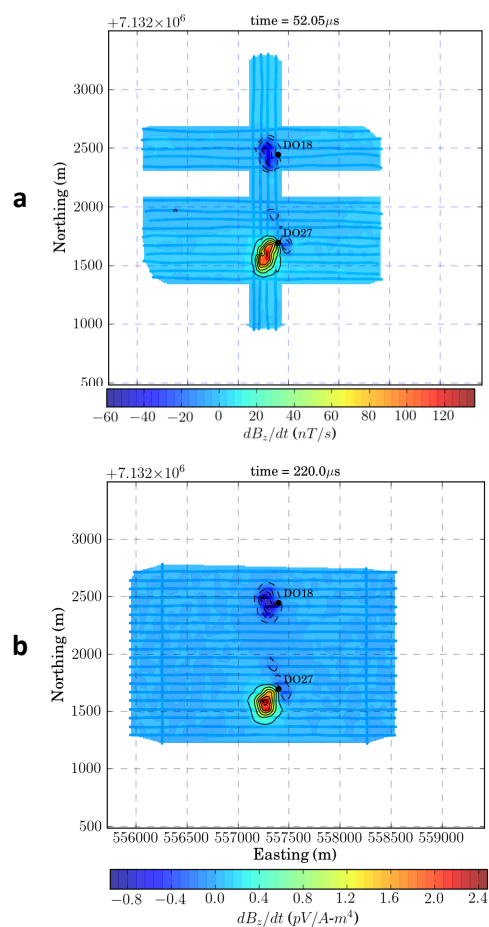


Figure 3: Interpolated  $\frac{\partial B_z}{\partial t}$  components from the (a) AeroTEM and (b) VTEM data set.

## Multi-EM systems inversion: Tli Kwi Cho complex

### 1D INVERSION

Each survey station is inverted independently using the UBC-EM1D codes assuming a simple layered Earth. It has been shown that measurements taken over 3D anomalies may yield artifacts (Farquharson et al., 2003; Yang and Oldenburg, 2012). Nevertheless, 1D inversions can provide representative structures in layered earth environments and information about a starting background model for 3D inversions. Importantly, the 1D inversions can also provide an indication about data quality and estimates of background noise levels needed for 3D inversions.

#### Laterally Constrained Inversion

Results from individual 1D inversions can be improved if information from neighboring stations can be incorporated as lateral constraints (Tartaras, 2005). Similar to the Laterally Constrained 1D Inversion (Auken and Christiansen, 2004), we propose an algorithm that manages information within a 3D framework, which can then be transferred to individual 1D inversions. Figure 4 presents our inversion workflow. The approach can efficiently account for varying topography, compute horizontal gradients and pass on geophysical and geological information through reference models and weight functions. Projection from the 1D inverted models to the 3D mesh is done using an inverse distance weighted average. The initial model is chosen by the inversion code as the *best-fitting half-space*. The starting model is updated after all 1D iterations are completed. This process is repeated until the model can predict the data up to a target misfit.

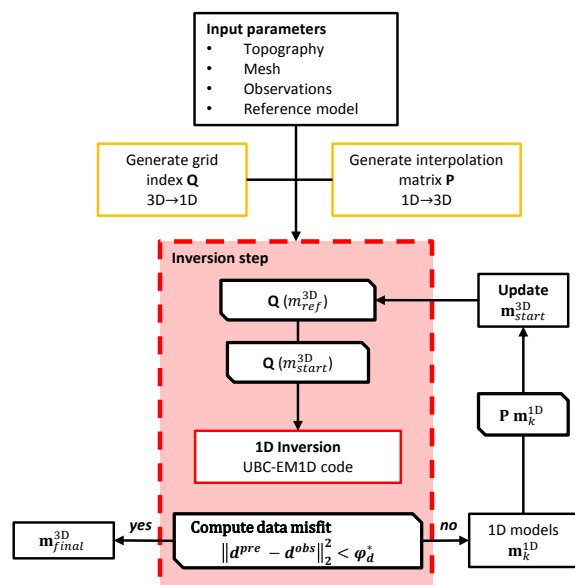


Figure 4: Inversion workflow used for the Laterally Constrained Inversion. The process is repeated until the model can predict the data up to a target misfit ( $\phi_d^*$ ).

#### Results

We implement our algorithm on the DIGHEM and AeroTEM data sets independently using the UBC-EM1DFM and EM1DTM

inversion codes. Only time channels with positive data were inverted from the AeroTEM data. Recovered 3D models from the DIGHEM and AeroTEM systems seem to agree fairly well near surface as shown on Figure 5 and 6. The interpreted geological sections from (Doyle et al., 1999) have been overlaid onto the inverted conductivity models as reference. Both models accurately recover the lake sediment and till layer thickness. The model also put a deeper vertical conductivity high along the center of DO-27.

However, the two models do not agree on the vertical extent of DO-27 and the actual conductivity values. The inverted model using the DIGHEM data recovers a much deeper and less conductive anomaly than the time-domain systems. These discrepancies motivate the need to invert the data in 3D, which is currently being undertaken.

### SUMMARY

In this paper we have modified pre-existing 1D inversion algorithms to generate a laterally constrained inversion algorithm with smoother variations in the horizontal directions. We inverted two EM data sets over the Tli Kwi Cho kimberlite complex. Our algorithm works within a 3D framework, making it easier to account for topography and giving more flexibility for external geological and geophysical inputs. The recovered models agree well with the near surface geology interpreted from drill-hole data. Discrepancies at depth are indicative of a 3D conductivity distribution that cannot be accounted for by 1D inversion techniques. Future work will focus on the 3D inversion of these data. Recovering a conductivity model that can reproduce all three data sets will help refine our understanding of the TKC kimberlite complex. An important goal however, is to provide a conductivity model that is necessary for carrying out an IP inversion of this airborne data. That is the topic of the third poster.

### ACKNOWLEDGMENTS

We would like to thank UBC-GIF and its members for their participation in processing and inverting and interpreting the field data sets.

# Multi-EM systems inversion: Tli Kwi Cho complex

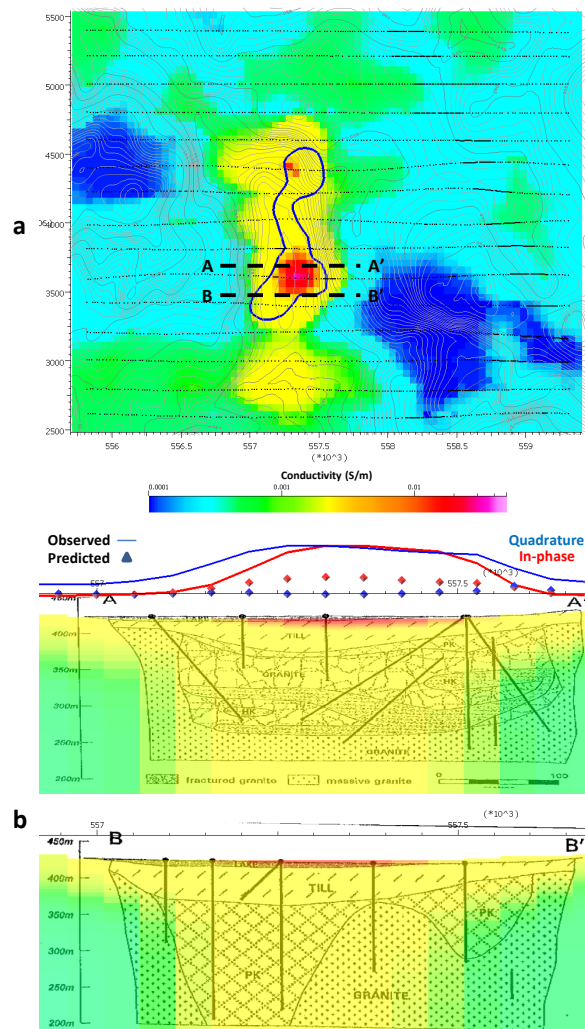


Figure 5: (a) Plan view ( $\sim 415$  m ASL) of the recovered conductivity model from the 1D inversion of the DIGHEM data set. (b) Vertical cross-sections at the same locations of the geological interpretations of Doyle *et al.* (1999). The inversion accurately recovered the depth of conductive lake sediments and till layer but did not recover the geometry of the kimberlite pipe. Observed and predicted data over the section are shown for reference. The inversion may have difficulty fitting the data due to IP effects.

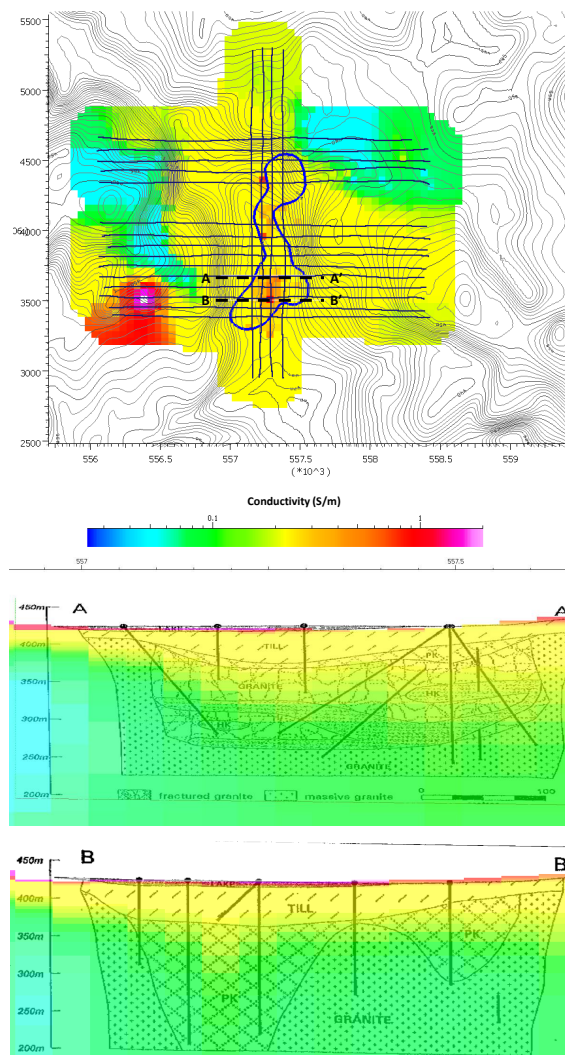


Figure 6: (a) Plan-view ( $\sim 415$  m ASL) of the recovered conductivity model from the 1D inversion of the AeroTEM data set. (b) Vertical cross-sections at the same locations of the geological interpretations of Doyle *et al.* (1999). The inversion accurately recovered the depth of the conductive overburden and sill layer, and also located the center of DO-27. The resolution of the inversion rapidly decreases with depth.

<http://dx.doi.org/10.1190/segam2014-1110.1>

## EDITED REFERENCES

Note: This reference list is a copy-edited version of the reference list submitted by the author. Reference lists for the 2014 SEG Technical Program Expanded Abstracts have been copy edited so that references provided with the online metadata for each paper will achieve a high degree of linking to cited sources that appear on the Web.

## REFERENCES

- Auken, E., and A. Christiansen, 2004, Layered and laterally constrained 2D inversion of resistivity data: *Geophysics*, **69**, no. 3, 752–761, <http://dx.doi.org/10.1190/1.1759461>.
- Boyko, W., N. Paterson, and K. Kwan, 2000, Aerotem: System characteristics and field results: Presented at the 2000 Annual Meeting of the CSEG.
- Coopersmith, H., J. Pell, and B. Smith, 2006, The importance of kimberlite geology in diamond deposit evaluation: A case study from the DO27/DO18 Kimberlite, NWT, Canada: Presented at the 8th International Kimberlite Conference.
- Doyle, B. J., K. Kivi, and S. B. H. Smith, 1999, The Tli Kwi Cho (DO27 and DO18) diamondiferous kimberlite complex, Northwest Territories, Canada: Proceedings of the 7th International Kimberlite Conference, 194–204.
- Farquharson, C., D. Oldenburg, and P. Routh, 2003, Simultaneous 1D inversion of loop-loop electromagnetic data for magnetic susceptibility and electrical conductivity: *Geophysics*, **68**, 1857–1869, <http://dx.doi.org/10.1190/1.1635038>.
- Jansen, J., and K. Witherly, 2004, The Tli Kwi Cho kimberlite complex, Northwest territories, Canada: A geophysical case study: 74<sup>th</sup> Annual Meeting and Exhibition, SEG, 1147–1150.
- Lord, C., and F. Barnes, 1954, NTS 76C Geology Map: Geological Survey of Canada.
- Reed, L., and K. Witherly, 2007, 50 years of kimberlite geophysics, a review: Fifth Decennial International Conference on Mineral Exploration, 679–689.
- Tartaras, E., 2005, LC1DINV: Laterally-Constrained 1D inversion for processing of airborne EM data: British Geological Survey: Internal Report.
- Weidelt, P., 1982, Response characteristics of coincident loop transient electromagnetic systems: *Geophysics*, **47**, 1325–1330, <http://dx.doi.org/10.1190/1.1441393>.
- Yang, D., and D. Oldenburg, 2012, Three-dimensional inversion of airborne time-domain electromagnetic data with applications to a porphyry deposit: *Geophysics*, **77**, no. 2, B23–B34, <http://dx.doi.org/10.1190/geo2011-0194.1>.